Strong Field Molecular Ionization in the Impulsive Limit: Freezing Vibrations with Short Pulses

Péter Sándor,[1] Vincent Tagliamonti,[1] Arthur Zhao,[1] Tamás Rozgonyi,[2] Matthias Ruckenbauer,[3]
Philipp Marquetand,[3] and Thomas Weinacht[1]

[1]*Department of Physics and Astronomy, Stony Brook University, Stony Brook, New York 11794-3800, USA*
[2]*Institute of Materials and Environmental Chemistry, Research Centre for Natural Sciences,
Hungarian Academy of Sciences, Magyar tudósok körútja 2, Budapest 1117, Hungary*
[3]*University of Vienna, Faculty of Chemistry, Institute of Theoretical Chemistry, Währinger Strasse 17, 1090 Wien, Austria*
(Received 11 November 2015; published 9 February 2016)

We study strong-field molecular ionization as a function of pulse duration. Experimental measurements of the photoelectron yield for a number of molecules reveal competition between different ionization continua (cationic states) which depends strongly on pulse duration. Surprisingly, in the limit of short pulse duration, we find that a single ionic continuum dominates the yield, whereas multiple continua are produced for longer pulses. Using calculations which take vibrational dynamics into account, we interpret our results in terms of nuclear motion and nonadiabatic dynamics during the ionization process.

Strong-field molecular ionization plays an important role in the generation of attosecond pulses and electron wave packets [1–4]. It can also be used to track excited state molecular dynamics and for molecular imaging [5–10]. A detailed understanding of the ionization dynamics is crucial for developing these frontier areas of molecular science [11]. In particular, with a push to improve time resolution in molecular dynamics experiments [12,13], generate multi-hole electron wave packets [14–18], and single attosecond pulses, it is important to understand how ionization depends on the duration of the strong-field driving pulse [19,20]. Here, we study strong-field molecular ionization as a function of pulse duration, going from several tens of fs to below 10 fs, where vibrational dynamics is frozen out (the "impulsive limit") [21]. Surprisingly, we find that, as we shorten the pulse duration from about 40 fs to less than 10 fs, there is a dramatic change in the photoelectron spectrum, which reflects a change in the combination of ionic continua that are accessed during the ionization process. We observe similar behavior in three different molecules (CH_2IBr, CH_2BrCl, and C_6H_5I) and demonstrate that the result depends more sensitively on pulse duration than spectral content. For CH_2IBr, we further interpret the experimental measurements in terms of calculations of strong-field molecular ionization which include vibrational dynamics on intermediate neutral states during the ionization process.

Our experimental apparatus consists of an amplified Ti:sapphire laser system, which produces 30 fs pulses with an energy of 1 mJ and a central wavelength of 780 nm. The pulses are focused into an Argon gas cell to create a filament and broaden the spectrum [22]. The pulses are compressed to near the transform limit with a 4-f grating compressor, and measured using a self-diffraction frequency-resolved optical gating (FROG) apparatus [23]. The broadest spectrum we produce is capable of supporting sub-6-fs pulses, and FROG measurements place an upper limit on the duration of the full bandwidth pulses of about 8–9 fs. The spectrum is cut using a variable slit in the grating compressor in order to obtain the variable bandwidth for the measurements below. The spectrum of the pulse is adjusted at the focusing element instead of the Fourier plane in order to avoid hard cutoffs at the edges of the spectrum, which would lead to a structured pulse in the time domain.

The linearly polarized laser beam crosses an effusive molecular beam in a vacuum chamber. Here, we generate electrons and ions, which are detected by accelerating them toward a dual stack of microchannel plates and phosphor screen with an electrostatic lens configured for velocity map imaging (VMI). The VMI lens produces a two-dimensional projection of the three-dimensional charged particle velocity distribution [24]. The hit locations on the phosphor screen from each laser shot are recorded and digitized by a CMOS camera which reads them into memory as separate images. The laser intensity is adjusted between 10–13 TW/cm^2 to keep the ionization yield roughly constant as the pulse duration is varied, yielding about 20 ± 10 electrons per laser shot. A computer algorithm extracts the hit locations from each image and synthesizes a single data image for any given laser pulse parametrization. This image is inverse-Abel transformed with the Gaussian basis-set expansion Abel transform method [25] and converted to a photoelectron spectrum. We focus on the yield that is generated $\pm 30°$ around the laser polarization direction. Integrating over all angles yields similar results, with slightly less contrast of the peaks.

Figure 1 shows photoelectron spectra for CH_2IBr as a function of pulse duration. For longer pulses (> 20 fs), two
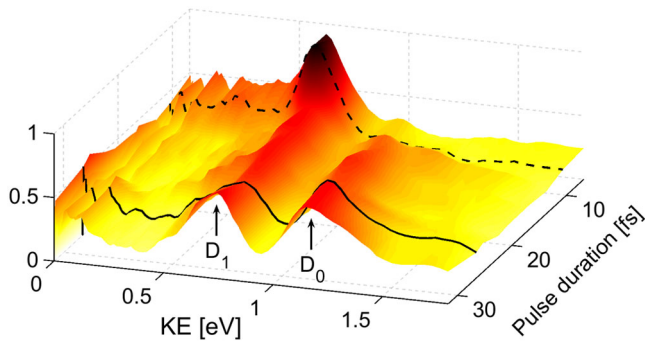
FIG. 1.   Photoelectron spectra [yield vs photoelectron kinetic energy (KE)] for ionization of CH_2IBr with different pulse durations.

FIG. 2.   Ratio of D_1/D_0 as a function of pulse duration τ for three different molecules.

peaks are visible: one at ≈ 1.2 eV and the other at ≈ 0.7 eV. Earlier work assigned these peaks to leaving the molecule in the first two states of the molecular cation: D_0 and D_1, respectively. The assignment of the spectrum to the molecular ions was verified using electron-ion coincidence spectroscopy [26]. While the yield from 0–0.2 eV and around 1.6 eV can be assigned to D_2/D_3 [26], we focus on the yield to D_0 and D_1 for simplicity here. Earlier work [27] also established that these peaks involve resonance enhancement via intermediate neutral states that Stark shift into resonance during the ionization process [28]. For longer pulses, ionization proceeds such that D_0 and D_1 are populated with roughly equal probability. However, as the pulse is shortened to below 12 fs, the yield for the D_0 peak diminishes and eventually becomes negligible compared to that of the D_1 peak. This is surprising given that the ionization potential for D_0 (9.7 eV) is lower than for D_1 (10.2 eV) [26], and that the bandwidth of a shorter pulse is broader.

We carried out similar measurements for other molecules and observed similar dynamics. Figure 2 shows the D_1 and D_0 ratio as a function of pulse duration for three different molecules: CH_2IBr, CH_2BrCl, and C_6H_5I. As the figure illustrates, all three molecules show similar behavior as a function of pulse duration. A shaded vertical bar marks the impulsive limit, corresponding to the C-H stretch vibrational period (≈ 11 fs—the shortest vibrational period for organic molecules) [29].

We now aim to interpret the measurements and determine whether the mechanism underlying the switching or control is driven by dynamics or spectral content. Since a shorter pulse duration requires a broader spectrum, it is natural to ask whether the suppression of ionization to D_0 is driven by new frequency components in the pulse, or rather by the pulse becoming shorter.

First, we address this question by making measurements with a series of narrow-band optical pulses with different central frequencies, adding up the photoelectron spectra with the appropriate weights, and comparing the result with the photoelectron spectrum measured for a short pulse that
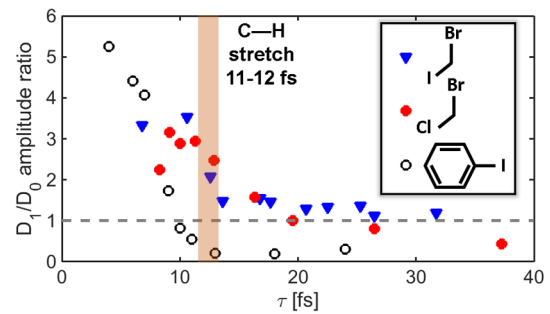
includes all the spectral components coherently. This idea is illustrated in Fig. 3. The top panel shows the optical spectrum of the short pulse and the weighted sum of the narrow optical spectra together, while the lower panel shows the resulting photoelectron spectra—one curve for the sum of the photoelectron spectra produced with narrow-band pulses and one curve for the photoelectron spectrum produced by a broadband pulse. The photoelectron spectra for the narrow-band pulses were added in proportion to the coefficients for the narrow-band optical spectra in forming the broadband spectrum as a linear combination. While the optical spectra are almost identical, there are significant differences between the two photoelectron spectra, indicating that it is not a single frequency in the pulse spectrum which drives the switching between ionic continua.

A second test that we performed was to vary the pulse duration while keeping the spectral content the same. This can be accomplished by placing a second-order spectral
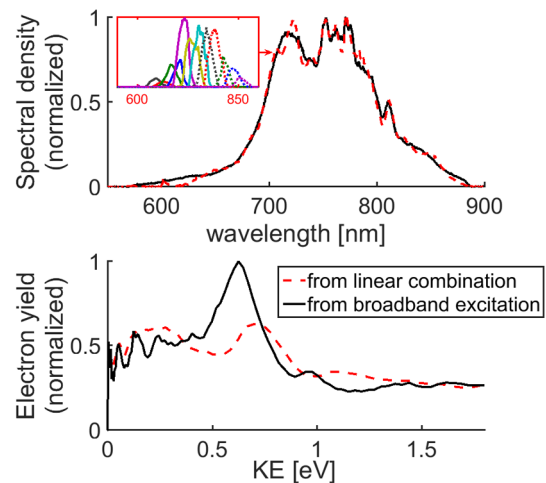

FIG. 3.   Top panel: Optical spectra for broadband pulse (solid black line) and the result of summing narrow-band spectra (dashed red line). Bottom panel: photoelectron spectra of CH_2IBr acquired with full bandwidth optical spectrum (solid black line), and the result of forming a linear combination of photoelectron spectra each acquired with narrow-band optical excitation (dashed red line). The latter are added in proportion to their spectral weights as shown in the inset and described in the text.

phase (chirp) on the broadband pulse, while varying the pulse energy to maintain a roughly constant yield. These results (to be presented in a forthcoming publication [30]) showed that the suppression of D_0 only takes place for a short pulse, corroborating the conclusion drawn above.

The observations described above suggest that there is some molecular dynamics which leads to both ionic states being populated, and if the pulse is shorter than the time scale for this dynamics, then only a single ionic state is populated. As the photoelectron spectrum is determined at the moment the electron is born in the continuum (i.e., it is not affected by possible subsequent dynamics in the molecular cation), we argue that the dynamics leading to the selectivity must be neutral dynamics, involving an excited neutral state en route to the ionization continuum. As in earlier work which established the importance of dynamically Stark-shifted resonances [31–33] in strong-field molecular ionization [26,33,34], our current intensity and wavelength dependent measurements indicate that neutral Rydberg states Stark shift into resonance during the ionization process. The correlation between a neutral Rydberg state and low lying states of the molecular cation is typically large for only a single cationic state with a similar configuration of the core—i.e., the Dyson norm for a given neutral state is large for a single low lying state of the cation, and close to zero for other states [35]. While Dyson correlations can be poor for low lying neutral states in strong-field ionization, they are better for higher lying states of the neutral where the electron which is removed during ionization does not interact with the ionic core very much and does not modify the core configuration. This means that once an intermediate neutral Rydberg state comes into resonance, it typically couples to a single ionic continuum [34]. Thus, for resonance-enhanced ionization to multiple continua, as is the case for a ≈ 40 fs pulse, multiple intermediate states must be involved in the ionization dynamics.

Our earlier work considered resonance enhanced ionization with separate uncoupled intermediate states for each ionization continua [34]. We extend this model to include coupling between the intermediate states as our new measurements suggest that separate uncoupled intermediate resonances cannot account for the pulse duration dependence we observe. If the bandwidth associated with different pulse durations were to select between different independent resonances, then one would expect to find a single ionic continuum favored for a long pulse (narrow bandwidth) rather than for a short pulse (broad bandwidth), since a shorter pulse contains a larger bandwidth, which would provide less selectivity between separate resonances. Furthermore, frequency-dependent measurements of the ionization yield such as the ones illustrated in Fig. 3 indicate that, when there is resonance enhancement of the ionization yield, then it is through a single neutral state

correlated with D_1. These measurements are discussed in detail in a separate publication [30].

While, in principle, both laser-driven resonance [6] and nonadiabatic dynamics could be responsible for coupling excited states, given the frequency-dependent measurements shown in Fig. 3, and motivated by earlier work [36], we focus on nonadiabatic dynamics as an explanation for the measurements shown in Figs. 1 and 2. We carry out calculations for CH_2IBr that include nonadiabatic coupling between excited states and which support the idea that molecular dynamics drives the switching between continua as a function of pulse duration.

Before modeling the strong-field ionization with numerical integration of the time-dependent Schrödinger equation, we carry out *ab initio* electronic structure calculation with multi-state complete-active-space perturbation theory of second order [37] in order to determine which electronic states play a crucial role in the ionization process. Details on the electronic structure calculations are given in the Supplemental Material [38]. The strong field ionization simulations are based on a simple model [27] which includes Stark-shifted intermediate neutral resonances. This model is now extended to include vibrational dynamics and nonadiabatic coupling between multiple intermediate neutral states, as considered in earlier calculations for weak (perturbative) laser fields [36]. We focus on CH_2IBr, for which we made the most detailed measurements and calculations.

As prior measurements suggest that resonance enhancement occurs at the five-photon level [27], we considered Rydberg states (R_0, R_1, and R_3) ≈ 8 eV above the ground state which are correlated (i.e., similar electronic configurations) with the low-lying ionic states (D_0, D_1, and D_3), and whose coordinate dependence follows those of the ionic states with which they are correlated. Then, we considered whether any nuclear coordinates led to coupling between these states. While the potential energy curves of the Rydberg states around 8 eV are largely parallel as a function of most vibrational coordinates, we found one mode (CH_2 wagging) along which motion leads to degeneracy (and, therefore, to population transfer via nonadiabatic coupling) between states correlated with D_0, D_1, and D_3. The potential energy curves of these states along this normal mode coordinate are shown in Fig. 4. In our calculations, population excited to R_1 (which, based on experimental measurements, is most strongly coupled to S_0 via the laser [30]) can quickly relax to R_3 and R_0 via rapid nuclear dynamics and nonadiabatic coupling. Based upon matches of the computed energy differences and similarities between the electronic states, R_0, R_1, and R_3 are coupled to D_0, D_1, and D_3, respectively. The strong-field ionization calculations produced the photoelectron spectrum as a function of pulse duration, as in the measurements. The energies of the resonant intermediate states were based on the electronic structure calculations and
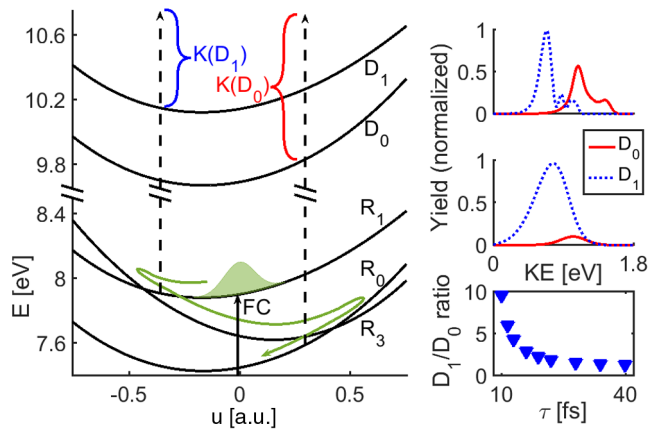
FIG. 4.   Left panel: calculated potential energy surfaces for CH_2IBr along the CH_2 wagging mode (u). FC: Franck-Condon point for excitation from the minimum of S_0 ($u = 0$). Upper right panel: calculated photoelectron spectra for 40 fs pulse. Middle right panel: calculated photoelectron spectra for 10 fs pulse. Bottom right panel: calculated D_1/D_0 yield ratio as a function of pulse duration τ.

comparison with experimental spectra. Laser parameters, such as the intensity, central frequency and pulse duration, were based on experimental parameters. The coupling strengths (multiphoton Rabi frequencies) are given in the Supplemental Material [38].

As the $S_0 \rightarrow R_1$ resonance dominates, population is initially transferred from S_0 to R_1. As Fig. 4 illustrates, motion along the CH_2 wagging mode couples states R_0, R_1, and R_3. The Franck-Condon (FC) point (minimum of S_0) is close to the R_1/R_3 crossing, leading to rapid population transfer from R_1 to R_3 ($\lesssim 5$ fs). Within ≈ 10 fs, the wave packet on R_3 can proceed to the R_3/R_0 crossing. Thus, for a long pulse, ionization can proceed to a mixture of the ionic states D_0, D_1, and D_3 coupled with the three neutral states R_0, R_1, and R_3. While our measurements show evidence of ionization to all three of these states, we concentrate on the competition between D_0 and D_1 because the measurements are cleanest for these states. In the limit of a short laser pulse, one might expect D_1 (which is correlated with R_1) to dominate the ionization yield since R_1 can shift into resonance and there is not sufficient time for the wave packet to move away from the FC on R_1 during the ionization. The ionization calculations aimed to test this hypothesis.

As the top right and middle panels of Fig. 4 illustrate, the photoelectron spectrum for a long pulse (40 fs) shows peaks corresponding to D_0 and D_1, whereas the photoelectron spectrum for a 10 fs pulse shows a single peak corresponding to D_1 only. This is in agreement with the results shown in Fig. 1, which shows two peaks corresponding to D_1 and D_0 for a long pulse and a single peak corresponding to D_1 for a short pulse. The bottom right panel of Fig. 4 shows a decreasing D_1/D_0 ratio as a function of pulse duration, in agreement with the results

shown in Fig. 2. One aspect of the measurements which is not reflected in the calculations is the width of the peaks in the PES as a function of pulse duration. The measurements show relatively narrow peaks for both short and long pulse durations, while the calculations show peaks which broaden as a function of decreasing pulse duration.

Our interpretation of the pulse duration dependence relies on neutral state resonances enhancing the ionization yield. Thus, one would expect that there is no change in the ionization yield for different ionic continua with pulse duration if there are no important resonances. In order to test this, we performed measurements of the photoelectron spectrum vs pulse duration in CS_2 for intensities where there are no intermediate resonances for our laser frequency. We also performed measurements in CH_2IBr for very low intensities where the intermediate states do not Stark shift into resonance. In both cases, we found that the photoelectron spectrum did not change substantially with pulse duration, as one would expect based on our interpretation which relies on dynamics in intermediate neutral states.

In conclusion, we study the state-resolved ionization yield as a function of pulse duration for several molecules and find that, for relatively long pulses, vibrational dynamics and nonadiabatic coupling between resonant intermediate states play an important role. For impulsive ionization with pulses less than 10 fs in duration, vibrational dynamics is frozen and no longer plays an important role in the ionization process. The transition between the two regimes is clearly visible in the photoelectron spectrum, in which a dramatic switching between single and multiple continua is observed. Surprisingly, resonance-enhanced ionization plays an important role for even the shortest pulses, containing nearly an octave optical bandwidth. Our results suggest that these considerations should be relevant for a broad range of molecules in strong laser fields.

[1] J. Levesque and P. B. Corkum, Can. J. Phys. **84**, 1 (2006).
[2] M. Krug, T. Bayer, M. Wollenhaupt, C. Sarpe-Tudoran, T. Baumert, S. S. Ivanov, and N. V. Vitanov, New J. Phys. **11**, 105051 (2009).
[3] P. Agostini and L. F. DiMauro, Rep. Prog. Phys. **67**, 813 (2004).
[4] E. Goulielmakis, Z.-H. Loh, A. Wirth, R. Santra, N. Rohringer, V. S. Yakovlev, S. Zherebtsov, T. Pfeifer, A. M. Azzeer, M. F. Kling et al., Nature (London) **466**, 739 (2010).
[5] T. Baumert, V. Engel, C. Meier, and G. Gerber, Chem. Phys. Lett. **200**, 488 (1992).
[6] D. Irimia and M. H. M. Janssen, J. Chem. Phys. **132**, 234302 (2010).

[7] J. L. Hansen, H. Stapelfeldt, D. Dimitrovski, M. Abu-samha, C. P. J. Martiny, and L. B. Madsen, Phys. Rev. Lett. **106**, 073001 (2011).

[8] D. Villeneuve, H. Niikura, N. Milosevic, T. Brabec, and P. Corkum, Nucl. Instrum. Methods Phys. Res., Sect. B **241**, 69 (2005).

[9] M. Meckel, D. Comtois, D. Zeidler, A. Staudte, D. Pavičić, H. C. Bandulet, H. Pépin, J. C. Kieffer, R. Dörner, D. M. Villeneuve et al., Science **320**, 1478 (2008).

[10] W. Li, A. A. Jaroń-Becker, C. W. Hogle, V. Sharma, X. Zhou, A. Becker, H. C. Kapteyn, and M. M. Murnane, Proc. Natl. Acad. Sci. U.S.A. **107**, 20219 (2010).

[11] M. Ivanov and O. Smirnova, Phys. Rev. Lett. **107**, 213605 (2011).

[12] A. Baltuška, T. Udem, M. Uiberacker, M. Hentschel, E. Goulielmakis, C. Gohle, R. Holzwarth, V. S. Yakovlev, A. Scrinzi, T. W. Hänsch et al., Nature (London) **421**, 611 (2003).

[13] P. Reckenthaeler, M. Centurion, W. Fuß, S. A. Trushin, F. Krausz, and E. E. Fill, Phys. Rev. Lett. **102**, 213001 (2009).

[14] S. V. Menon, J. P. Nibarger, and G. N. Gibson, J. Phys. B **35**, 2961 (2002).

[15] P. Johnsson, R. López-Martens, S. Kazamias, J. Mauritsson, C. Valentin, T. Remetter, K. Varjú, M. B. Gaarde, Y. Mairesse, H. Wabnitz et al., Phys. Rev. Lett. **95**, 013001 (2005).

[16] M. F. Kling, C. Siedschlag, A. J. Verhoef, J. I. Khan, M. Schultze, T. Uphues, Y. Ni, M. Uiberacker, M. Drescher, F. Krausz et al., Science **312**, 246 (2006).

[17] B. K. McFarland, J. P. Farrell, P. H. Bucksbaum, and M. Gühr, Science **322**, 1232 (2008).

[18] B. Bergues, M. Kübel, N. G. Johnson, B. Fischer, N. Camus, K. J. Betsch, O. Herrwerth, A. Senftleben, A. M. Sayler, T. Rathje et al., Nat. Commun. **3**, 813 (2012).

[19] G. Sansone, E. Benedetti, F. Calegari, C. Vozzi, L. Avaldi, R. Flammini, L. Poletto, P. Villoresi, C. Altucci, R. Velotta et al., Science **314**, 443 (2006).

[20] M.-C. Chen, C. Mancuso, C. Hernández-García, F. Dollar, B. Galloway, D. Popmintchev, P.-C. Huang, B. Walker, L. Plaja, A. A. Jaroń-Becker et al., Proc. Natl. Acad. Sci. U.S.A. **111**, E2361 (2014).

[21] X. Xie, E. Lötstedt, S. Roither, M. Schöffler, D. Kartashov, K. Midorikawa, A. Baltuška, K. Yamanouchi, and M. Kitzler, Sci. Rep. **5**, 12877 (2015).

[22] G. Stibenz, N. Zhavoronkov, and G. Steinmeyer, Opt. Lett. **31**, 274 (2006).

[23] R. Trebino, K. W. DeLong, D. N. Fittinghoff, J. N. Sweetser, M. A. Krumbügel, B. A. Richman, and D. J. Kane, Rev. Sci. Instrum. **68**, 3277 (1997).

[24] A. T. J. B. Eppink and D. H. Parker, Rev. Sci. Instrum. **68**, 3477 (1997).

[25] V. Dribinski, A. Ossadtchi, V. A. Mandelshtam, and H. Reisler, Rev. Sci. Instrum. **73**, 2634 (2002).

[26] P. Sándor, A. Zhao, T. Rozgonyi, and T. Weinacht, J. Phys. B **47**, 124021 (2014).

[27] W. D. M. Lunden, P. Sándor, T. C. Weinacht, and T. Rozgonyi, Phys. Rev. A **89**, 053403 (2014).

[28] We note that intermediate neutral states can play an important role even for very short pulses, where the

resonance condition is only met for a relatively short time, provided that there is sufficiently strong coupling.

[29] Y. Yu, K. Lin, X. Zhou, H. Wang, S. Liu, and X. Ma, J. Phys. Chem. C **111**, 8971 (2007).

[30] V. Tagliamonti, P. Sándor, A. Zhao, T. Rozgonyi, and T. Weinacht (to be published).

[31] G. N. Gibson, R. R. Freeman, T. J. McIlrath, and H. G. Muller, Phys. Rev. A **49**, 3870 (1994).

[32] R. R. Freeman, P. H. Bucksbaum, H. Milchberg, S. Darack, D. Schumacher, and M. E. Geusic, Phys. Rev. Lett. **59**, 1092 (1987).

[33] G. N. Gibson, R. R. Freeman, and T. J. McIlrath, Phys. Rev. Lett. **69**, 1904 (1992).

[34] W. D. M. Lunden, D. Geißler, P. Sándor, T. C. Weinacht, and T. Rozgonyi, Phys. Rev. A **89**, 053404 (2014).

[35] M. Spanner, S. Patchkovskii, C. Zhou, S. Matsika, M. Kotur, and T. C. Weinacht, Phys. Rev. A **86**, 053406 (2012).

[36] M. Seel and W. Domcke, J. Chem. Phys. **95**, 7806 (1991).

[37] J. Finley, P.-A. Malmqvist, B. O. Roos, and L. Serrano-Andrés, Chem. Phys. Lett. **288**, 299 (1998).

[38] See Supplemental Material at http://link.aps.org/supplemental/10.1103/PhysRevLett.116.063002 for FROG spectrum of the experimental pulses and for details of ab initio computations and wavepacket dynamics for CH_2BrI, which includes Refs. [23,36,37,39–54].

[39] M. J. Frisch et al., GAUSSIAN 2003, Gaussian Inc., 2003.

[40] P. J. Stephens, F. J. Devlin, C. F. Chabalowski, and M. J. Frisch, J. Phys. Chem. **98**, 11623 (1994).

[41] K. A. Peterson, D. Figgen, E. Goll, H. Stoll, and M. Dolg, J. Chem. Phys., **119**, 11113 (2003).

[42] J. González-Vázquez, L. González, S. R. Nichols, T. C. Weinacht, and T. Rozgonyi, Phys. Chem. Chem. Phys. **12**, 14203 (2010).

[43] K. Andersson, P.-A. Malmqvist, and B. O. Roos, J. Chem. Phys., **96**, 1218 (1992).

[44] F. Aquilante, L. De Vico, N. Ferré, G. Ghigo, P.-A Malmqvist, P. Neogrády, T. B. Pedersen, M. Pitonak, M. Reiher, B. O. Roos, L. Serrano-Andrés, M. Urban, V. Veryazov, and R. Lindh, J. Comput. Chem. **31**, 224 (2010).

[45] M. Reiher, Theor. Chem. Acc. **116**, 241 (2006).

[46] P.-O. Widmark, P.-A. Malmqvist, and B. O. Roos, Theor. Chim. Acta, **77**, 291 (1990).

[47] B. O. Roos, R. Lindh, P.-A. Malmqvist, V. Veryazov, and P.-O. Widmark, J. Phys. Chem. A, **108**, 2851 (2004).

[48] K. Kaufmann, W. Baumeister, and M. Jungen, J. Phys. B, **22**, 2223 (1989).

[49] C. M. Marian and U. Wahlgern, Chem. Phys. Lett. **251**, 357 (1996).

[50] A. F. Lago, J. P. Kercher, A. Bódi, B. Sztáray, B. Miller, D. Wurzelmann, and T. Baer, J. Phys. Chem. A **109**, 1802 (2005).

[51] Penner and Amirav, J. Chem. Phys. **93**, 8576 (1990).

[52] T. Rozgonyi, A. Glass, and T. Feurer, J. Appl. Phys., **88**, 2936 (2000).

[53] C. Trallero-Herrero, D. Cardoza, T. C. Weinacht, and J. L. Cohen, Phys. Rev. A **71**, 013423 (2005).

[54] W. D. M. Lunden, P. Sándor, T. C. Weinacht, and T. Rozgonyi, Phys. Rev. A **89**, 053403 (2014).